Int. J. Electrochem. Sci., 11 **(2016)** 10135 – 10149, doi: 10.20964/2016.12.20

International Journal of
ELECTROCHEMICAL
SCIENCE
www.electrochemsci.org

Investigation of Diantipyrylmethane as Corrosion Inhibitor for Mild Steel in Sulfuric Acid Solution

Lijuan Gong[1,*], *Kangquan Qiao*[2,3]

[1] College of Bioengineering, Sichuan University of Science & Engineering, Zigong 643000, P. R. China
[2] Analysis and Testing Center, Sichuan University of Science & Engineering, Zigong 643000, P. R. China
[3] Material Corrosion and Protection Key Laboratory of Sichuan Province, Zigong 643000, P. R. China
[*]E-mail: g_ljuan@163.com

Received: 27 July 2016 / *Accepted:* 11 September 2016 / *Published:* 10 November 2016

The corrosion inhibition performances of Diantipyrylmethane (DAM) for mild steel in 0.5 M H_2SO_4 were investigated using weight loss, electrochemical impedance spectroscopy (EIS), potentiodynamic polarization, scanning electron microscope (SEM) and quantum chemical calculation. The obtained results reveal that DAM acts as a mixed-type inhibitor with a predominantly anodic reaction, and the inhibition efficiency increases with increasing inhibitor concentration whereas decreases with increasing temperature. The adsorption of DAM on steel surface is found to obey Langmuir isotherm, and the adsorption mechanism is mixed physical and chemical adsorption. The results of quantum chemical calculation demonstrate that pyrazolone rings within molecular structure of DAM play a dominant role in corrosion inhibition of mild steel.

Keywords: Diantipyrylmethane, Mild steel, Acid Corrosion

1. INTRODUCTION

Corrosion inhibitors are commonly used as additives to inhibit the corrosion of metals in liquid medium[1]. Heterocyclic compounds are identified as one of the most effective inhibitors for steel corrosion in acid medium, these inhibitors can adsorb on the steel surface through nitrogen, sulfur, phosphorus, oxygen, triple bond, conjugated double bond, and/or aromatic rings in their own molecular structures[2-3]. In addition, a lot of N-heterocyclic compounds have been considered as excellent inhibitors for steel corrosion in acid medium, such as imidazoline derivatives[4], pyridine derivatives [5], Pyrimidine derivatives[6], pyrazolone derivatives[7-13], and so on.

As an important kind of pyrazolone derivatives, DAM containing two pyrazolone rings and two phenyls can be deemed as a good potential inhibitor for metal corrosion in acid medium, in this case, these functional groups may be used as active sites for bonding with metal surface.

Generally, DAM as an inexpensive agent is employed for determination, separation and purifiction of metal ions [14-15]. So far there is still a lack of systematic research on the corrosion inhibition properties of DAM for steel in acid medium. Accordingly, in this paper, the corrosion inhibition effects of DAM on mild steel in 0.5 M H_2SO_4 was studied using weight loss, electrochemical measurements, SEM and quantum chemical calculation, and thermodynamic parameters and kinetic parameters relating to the corrosion and adsorption process were evaluated in detail.

2. EXPERIMENTAL

2.1 Material and sample preparation

The chemical composition (wt %) of Mild steel used in this study is as follow: C (0.17%), Si (0.30%), Mn (0.20%), P (0.005%), S (0.005%), and Fe for balance. The mild steel coupons used for weight loss test and surface analysis were cut into 50 mm × 20 mm × 2 mm, 10 mm × 10 mm × 2 mm, respectively. The working electrode is a steel rod embedded in epoxy resin and the working area is 0.785 cm^2. Prior to all experiments, the working surface of mild steel was mechanically abraded using metallographic abrasive paper to 1200 grit.

All chemical reagents were of analytical grade. The aggressive medium of 0.5 M H_2SO_4 solution was prepared with 98 % H_2SO_4 and distilled water. DAM was obtained from Shanghai Aladdin Biochemical Technology Co., Ltd. Fig. 1 shows the molecular structure of DAM, which can easily dissolve in 0.5 M H_2SO_4 solution.

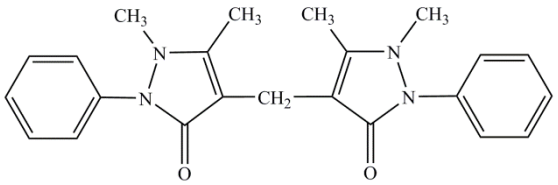

Figure 1. Molecular structure of DAM {IUPAC name: 4-[(1,5-dimethyl-3-oxo-2-phenylpyrazol -4-yl)methyl]-1,5-dimethyl-2-phenylpyrazol-3-one}

2.2. Weight loss measurements

Cleaned and weighed mild steel coupons were immersed in 0.5 M H_2SO_4 solution without and with various concentrations of DAM for 6 h at different temperatures, respectively. Then the mild steel coupons were cleaned by distilled water and acetone, dried and weighed at room temperature.

Experiments were carried out in triplicate, and the average weight loss of coupons were calculated and used as results.

2.3. Electrochemical measurements

An integrated three-electrode system including platinum electrode, saturated calomel electrode (SCE) and mild steel electrode was employed for electrochemical measurements using PARSTAT2273 electrochemical workstation (Princeton Applied Research). Before starting the electrochemical measurements, each working electrode was immersed in the test solution for 30 min to reach a steady open circuit potential (OCP). EIS measurements were implemented at OCP over the frequency range of 100 kHz to 0.01 Hz with amplitude of 5 mV. EIS data was analysed by ZSimpWin software. The potentiodynamic polarization measurements were implemented in the potential range of −250 to +250 mV versus OCP at a scan rate of 0.5 mV/s, the polarization data was analysed by PowerSuite software.

2.4. SEM measurements

Cleaned and weighed mild steel coupons were exposed to 0.5 M H_2SO_4 solution without and with 40 μM DAM at 298K for 3 h. The surface morphology analysis of these coupons before and after immersion were investigated by SEM (Tescan Vega33, Czech Republic) at 20.0 kV.

2.5. Calculation method

Quantum chemical calculation was performed by Gaussian 09 program software. The molecular structure of DAM was geometrically optimized by density functional theory (DFT) using B3LYP functional with 6-31G basis set. Quantum chemical parameters containing the total energy, the energy of lowest occupied molecular orbital (E_{LUMO}), the energy of highest occupied molecular orbital (E_{HOMO}), the energy gap ($\Delta E = E_{LUMO} - E_{HOMO}$), Mulliken charge, and the dipole moment (μ) were calculated and discussed.

3. RESULTS AND DISCUSSION

3.1. Weight loss

The weights of mild steel coupons after immersion in 0.5 M H_2SO_4 solution without and with different concentrations of DAM for 6 h at various temperatures were measured. Thus, the corrosion rate (v, g•m^{-2}•h^{-1}) and the inhibition efficiency (η, %) can be calculated as follows [16]:

$$v = \frac{w}{S \cdot t} \quad (1)$$

$$\eta\ (\%) = \frac{(v_0 - v_i)}{v_0} \times 100\ \% \quad (2)$$

Where, w is the average weight loss of three parallel coupons, S is the surface area of each coupon, t is immersion time, v_0 and v_i are the corrosion rates without and with DAM respectively. The obtained results were given in Fig. 2.

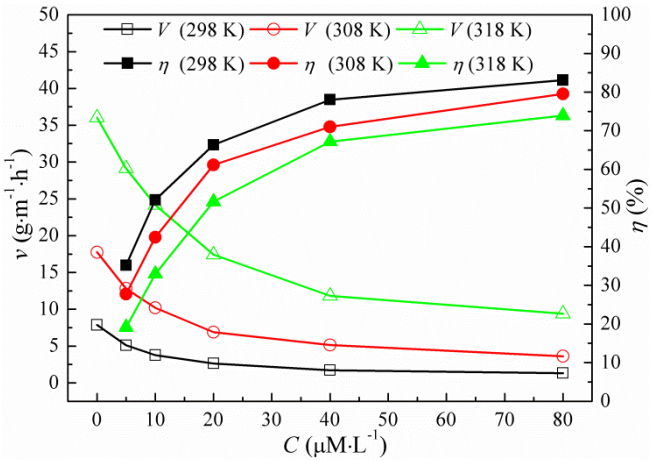

Figure 2. The results of weight loss for mild steel in 0.5 M H_2SO_4 without and with various concentrations of DAM at different temperatures

As shown in Fig. 2, the corrosion rate decreases with increasing DAM concentration at 298, 308 and 318 K, respectively, as a result, the inhibition efficiency increases with the presence of higher DAM concentration. It is obvious that DAM molecules may effectively absorb on steel surface and inhibit steel corrosion in 0.5 M H_2SO_4 at the temperature range of 298 - 318K[17]. However, when DAM concentration exceed 40 μM the growth rate of the inhibition efficiency obviously decreases, which illustrates that the absorption of DAM molecules on steel surface at high DAM concentration gradually tend to stable[18].

3.2 Adsorption isotherm and thermodynamic parameters

Generally, the organic molecules inhibit steel corrosion in acid medium by their adsorption on steel/solution interface. In fact, an appropriate adsorption isotherm may accurately exhibit the inhibitor adsorption process. In this case, a series of adsorption isotherms were used to fit weight loss results at different temperatures. Consequently, the adsorption behavior of DAM at each temperature obeys Langmuir adsorption isotherm[19]:

$$\frac{C}{\theta} = \frac{1}{K_{ads}} + C \quad (3)$$

Where C is DAM concentration, θ is equal to η obtained by weight loss method, which may represent the degree of DAM coverage on steel surface, K_{ads} is the equilibrium. Subsequently, K_{ads} may

be applied to calculate the standard free energy of adsorption (ΔG^0_{ads}), enthalpy (ΔH^0_{ads}) and entropy (ΔS^0_{ads}) of adsorption process according to the following equations [20]:

$$\Delta G^0_{ads} = -RT\ln(55.5\,K_{ads}) \quad (4)$$

$$\ln K_{ads} = \frac{\Delta H^0_{ads}}{RT} + \text{constant} \quad (5)$$

$$\Delta S^0_{ads} = \frac{\Delta H^0_{ads} - \Delta G^0_{ads}}{T} \quad (6)$$

Where R is the molar gas constant (8.314 J•mol^{-1}•K^{-1}) and T is the absolute temperature (K).

The plots of C versus C/θ yield straight lines at various temperatures, as shown in Fig.3. All correlation coefficients (R^2) and slopes at various temperatures are very close to 1, indicating that the adsorption of DAM on mild steel surface follows Langmuir adsorption isotherm and DAM molecule approximately occupy one site[21].

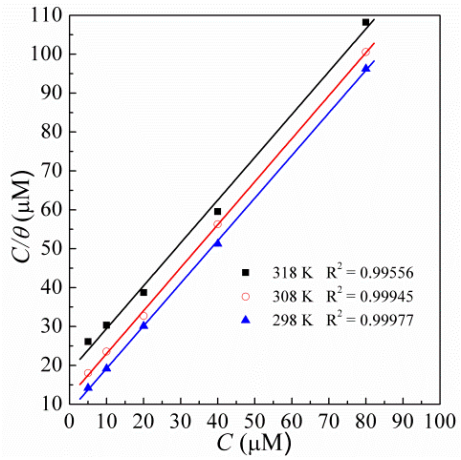

Figure 3. Langmuir adsorption isotherm for mild steel in 0.5 M H_2SO_4 with various concentrations of DAM at different temperatures

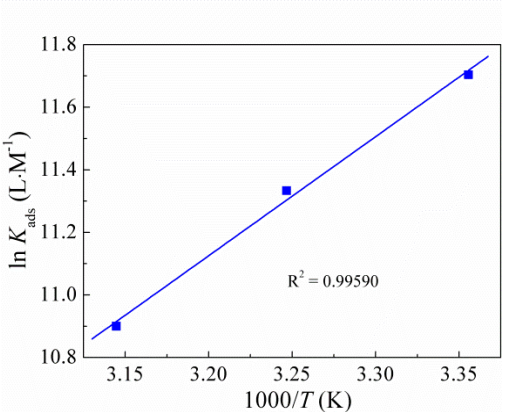

Figure 4. The relationship between ln K_{ads} and $1/T$ for mild steel in 0.5 M H_2SO_4 with various concentrations of DAM

According to equation (5), the plot of ln K_{ads} versus 1/T yields a straight line, as shown in Fig. 4, thus, the adsorption parameters containing K_{ads} , ΔG^0_{ads}, ΔH^0_{ads} and ΔS^0_{ads} are calculated and given in Table 1. The large values of K_{ads} and the relatively negative values of ΔG^0_{ads} demonstrate that DAM molecule has the strong interaction with steel surface by spontaneous adsorption in 0.5 M H_2SO_4 solution. The K_{ads} values decrease with the increase of temperature, in this case, the absorption of DAM molecule on steel surface is more difficult at higher temperature[13]. The ΔG^0_{ads} values at different temperatures are in the range of -36 to -39 kJ/mol, implying that the adsorption mechanism of DAM on mild steel surface is mixed physical and chemical adsorption[22]. The negative values of ΔH^0_{ads} show that the adsorption of DAM is an exothermic process, and the positive values of ΔS^0_{ads} demonstrate that the randomness increases with the replacement of adsorbed water molecules by DAM molecules on mil steel surface[19].

Table 1. Thermodynamic parameters for mild steel in 0.5 M H_2SO_4 with various concentrations of DAM at different temperatures

T (K)	K_{ads} (L·mol^{-1})	ΔG^0_{ads} (KJ·mol^{-1})	ΔH^0_{ads} (KJ·mol)	ΔS^0_{ads} (J·mol^{-1}·K^{-1})
298	120997	-38.97	-31.63	24.62
308	83546	-38.05	-31.63	20.84
318	54153	-36.97	-31.63	16.80

3.3. Activation parameters

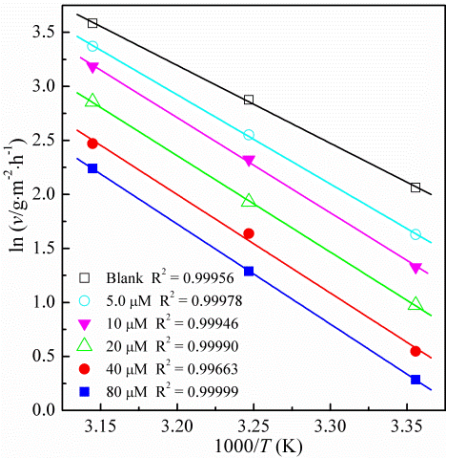

Figure 5. Arrhenius plots for mild steel in 0.5 M H_2SO_4 without and with various concentrations of DAM

The inhibition performance of DAM may be dramatically influenced by temperature. The effect of temperature on the corrosion rate of mild steel in 0.5 M H_2SO_4 solution was discussed using Arrhenius and transition state equations[23-24]:

$$\ln v = -\frac{E_a}{RT} + \ln \lambda \quad (7)$$

$$\ln v/T = \ln \frac{R}{Nh} + \frac{\Delta S_a}{R} - \frac{\Delta H_a}{RT} \quad (8)$$

Where λ is the pre-exponential factor, h is the plank's constant, N is Avogadro's number, E_a is the apparent activation energy, ΔS_a is the apparent entropy of activation, ΔH_a is the apparent enthalpy of activation.

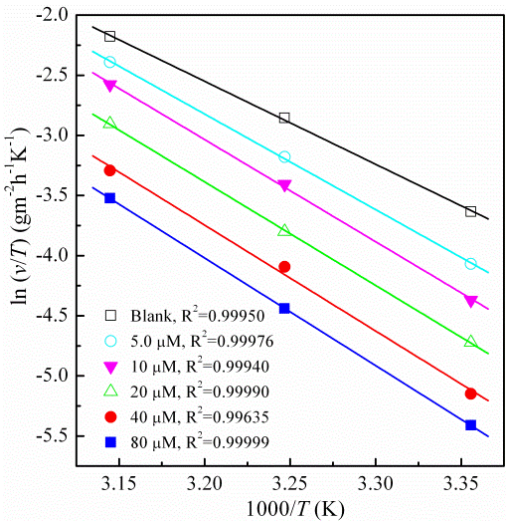

Figure 6. Transition state plots for mild steel in 0.5 M H_2SO_4 without and with various concentrations of DAM

As expected, according to equation (7) and (8), the obtained plots in Fig. 5 and 6 yield straight lines separately, thus these parameters including E_a, ΔH_a and ΔS are calculated and listed in Table 2, ΔS is the difference value between $\Delta S_{a,i}$ (ΔS_a obtained from DAM solution) and $\Delta S_{a,0}$ (ΔS_a obtained from blank solution). The E_a values are greater in DAM solution than in blank solution, indicating that steel dissolution is unfavorable in DAM solution due to the adsorption of inhibitor molecules[25]. Furthermore, the ΔS values are greater than zero in DAM solution, implying that the randomness increases during the formation process of activated complex [26].

Table 2. Activation parameters for mild steel in 0.5 M H_2SO_4 in the absence and presence of various concentrations of DAM

C (μM)	Ea (kJ·mol^{-1})	ΔHa (kJ·mol^{-1})	$\Delta S = \Delta S_{a,i} - \Delta S_{a,0}$ (J·mol^{-1}·K^{-1})
Blank	59.94	57.38	0
5	68.66	66.10	25.65
10	73.19	70.63	38.38
20	74.17	71.61	38.57
40	75.78	73.23	40.75

80	76.99	74.43	42.34

3.4 Electrochemical impedance spectroscopy (EIS)

Nyquist and Bode diagrams for mild steel in 0.5 M H_2SO_4 solution at 298 K without and with different concentrations of DAM were given in Fig. 7.

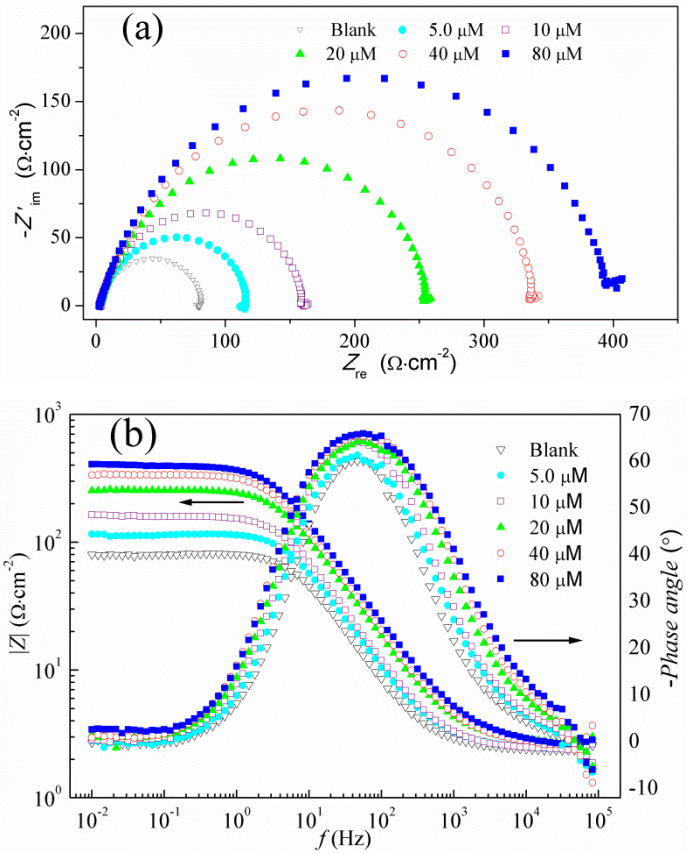

Figure 7. Nyquist (a) and Bode diagrams (b) for mild steel in 0.5 M H_2SO_4 in the absence and presence of DAM at 298 K

It is obvious from Fig. 7 that the diameters of capacitive loop of Nyquist plots at high frequency (HF) significantly enhance with the increase of DAM concentration, indicating that the corrosion process of mild steel is mainly charge-transfer controlled [27]. Nyquist plots show depressed semicircular appearance, the deviations from ideal semicircles are usually attributed to the frequency dispersion and the non-homogeneity of mild steel surface [28].

Electrical equivalent circuit given in Fig. 8 are used to simulate EIS data by ZSimpWin software. In the circuit, R_s is the solution resistance, R_{ct} is the charge transfer resistance corresponding to the diameter of Nyquist plot and inhibition efficiency (η), CPE is the constant phase element, which may be calculated as follows[29]:

$$Z_{\mathrm{CPE}} = \frac{1}{Y_0(j\omega)^n} \quad (9)$$

where Y_0 is the CPE constant, n is the phase , j is the imaginary unit, ω is the angular frequency. Accordingly, the C_{dl} value may be calculated using the following equation[29-30]:

$$C_{\mathrm{dl}} = Y_0(\omega_{\max})^{n-1} = Y_0(2\pi f_{\mathrm{zim-max}})^{n-1} \quad (10)$$

where ω_{max} corresponding to $f_{\text{zim-max}}$ is the maximum value of ω at the imaginary part (zim-max). Thus, the values of R_s, R_{ct}, Y_o, n, C_{dl} and η are given in Table 3. the η values may be calculated using the following equation[29]:

$$\eta\,\% = \frac{(R_{\mathrm{ct},0} - R_{\mathrm{ct,i}})}{R_{\mathrm{ct},0}} \times 100\,\% \quad (11)$$

where $R_{ct,0}$ and $R_{ct,i}$ are the R_{ct} values in the absence and presence of DAM respectively.

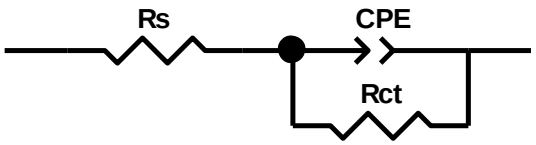

Figure 8. Equivalent circuit model used to simulate EIS data

Table 3. EIS parameters for mild steel in 0.5 M H_2SO_4 without and with various concentrations of DAM at 298 K

C (μM)	R_s ($\Omega\cdot cm^{-2}$)	$Y_0\times10^6$ ($S\cdot s^n\cdot cm^{-2}$)	n	C_{dl} ($\mu F\cdot cm^{-2}$)	R_{ct} ($\Omega\cdot cm^{-2}$)	η (%)
Blank	2.4	461.1	0.8756	289.0	79.6	
5	2.5	401.3	0.8566	240.7	115.5	31.08
10	2.5	337.5	0.8628	212.5	161.0	50.56
20	2.8	250.1	0.8407	150.7	259.8	69.36
40	2.8	220.7	0.8413	137.4	344.8	76.91
80	2.7	199.1	0.8287	119.3	409.2	80.55

As can be seen from Table 3, the R_{ct} values increase with increasing DAM concentration while the C_{dl} values exhibit opposite dependence. The increase of R_{ct} values corresponding to the inhibition efficiencies should be attributed to the extension of coverage of absorbed DAM molecules on mild steel surface. The values of C_{dl} values should due to the reduction of the local dielectric constant and/or the increase of the thickness of the electrical double layer with replacement of water molecules and other ions on steel surface/solution by DAM molecules[31]. The n values are close to 1 suggesting that CPE is related to capacitive, however, the n values decrease with increasing DAM concentration, which should be derived from the change of adsorption film of DAM molecules[32].

3.5 Potentiodynamic polarization

Potentiodynamic polarization curves for mild steel in 0.5 M H_2SO_4 without and with various concentrations of DAM at 298 K are shown in Fig. 9, respectively. The corresponding parameters

containing the corrosion potential (E_{corr}), the cathodic Tafel slope (β_c), the anodic Tafel slope (β_a), the inhibition efficiency (η) and the corrosion current density (j_{corr}) were listed in Table 4. The η values were calculated using the following equation[33]:

$$\eta\ \% = \frac{(j_{corr,0} - j_{corr,i})}{j_{corr,0}} \times 100\ \% \quad (12)$$

where $j_{corr,0}$ and $j_{corr,i}$ are the j_{corr} values in the absence and presence of DAM respectively.

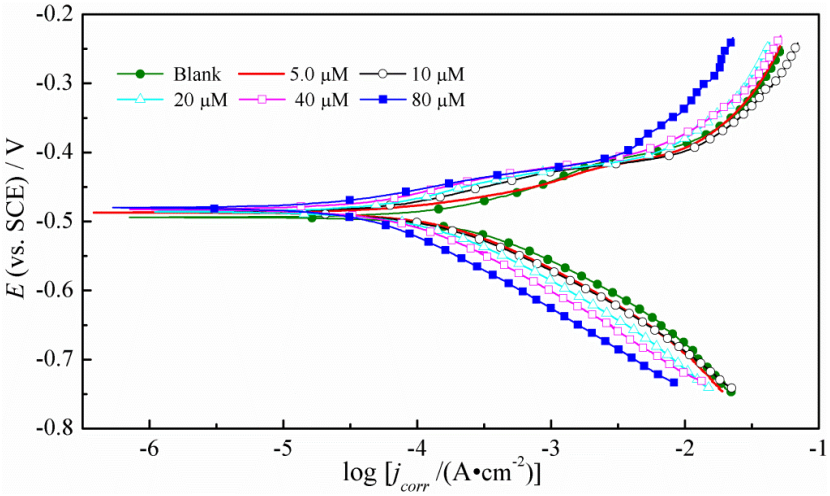

Figure 9. Polarization curves for mild steel in 0.5 M H_2SO_4 without and with various concentrations of DAM at 298 k

Table 4. Polarization parameters for mild steel in 0.5 M H_2SO_4 without and with various concentrations of DAM at 298 K

C (μM)	E_{corr} (V)	β_c (mV•dec^{-1})	β_a (mV•dec^{-1})	j_{corr} (μA•cm^{-2})	η (%)
Blank	-0.494	105.74	84.91	255.9	—
5	-0.487	106.18	59.00	172.0	32.79
10	-0.487	105.22	55.87	123.6	51.70
20	-0.486	105.53	55.46	86.1	66.35
40	-0.483	104.90	47.57	58.8	77.02
80	-0.480	107.12	40.91	46.8	81.71

It is obvious from Fig. 9 and Table 4 that the cathodic and anodic current curves both shift lower current density with increasing DAM concentration, indicating that DAM can simultaneously inhibit hydrogen evolution and anodic dissolution processes on steel surface in H_2SO_4 solution[34]. All corrosion potentials shift to more positive values with the addition of DAM but the potential differences between DAM solutions and blank solution are less than 0.4 V, moreover, the anodic Tafel slopes significantly decline with increasing DAM concentration while the cathodic Tafel slopes are

almost coincident. The above results reveal that DAM can be considered as a mixed-type inhibitor with more a predominantly anodic reaction[35]. In addition, the change tendency of the η values coming from potentiodynamic polarization is in good correspondence with the results of weight loss and EIS tests.

3.6 Surface characterization

To evaluate the corrosion state of mild steel surface exposed to corrosive medium at 298K, a superficial analysis was performed using SEM images. As seen from Fig. 10, the surface of steel immersed in 80 µM DAM [Fig. 10 (c)] exhibits less damage than in blank solution [Fig. 10 (b)], which should be attibuted to the strong adsorption of DAM molecules on steel surface[36]. Therefore, DAM should be considered as an effective corrosion inhibitor for mild steel in acid medium.

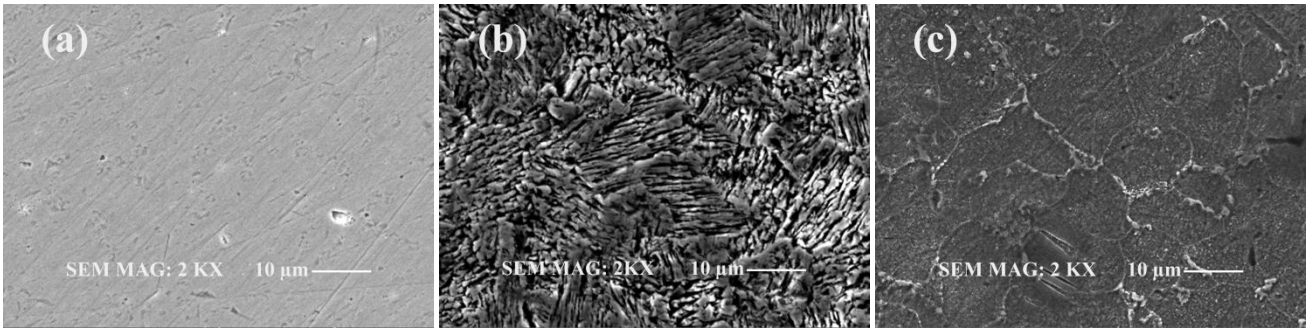

Figure 10. SEM micrographs of mild surface: (a) no immersion, (b) after 3 h immersion in 0.5 M H_2SO_4, (c) after 3 h immersion in 0.5 M H_2SO4 + 80 µM DAM.

3.7 Quantum chemical calculations

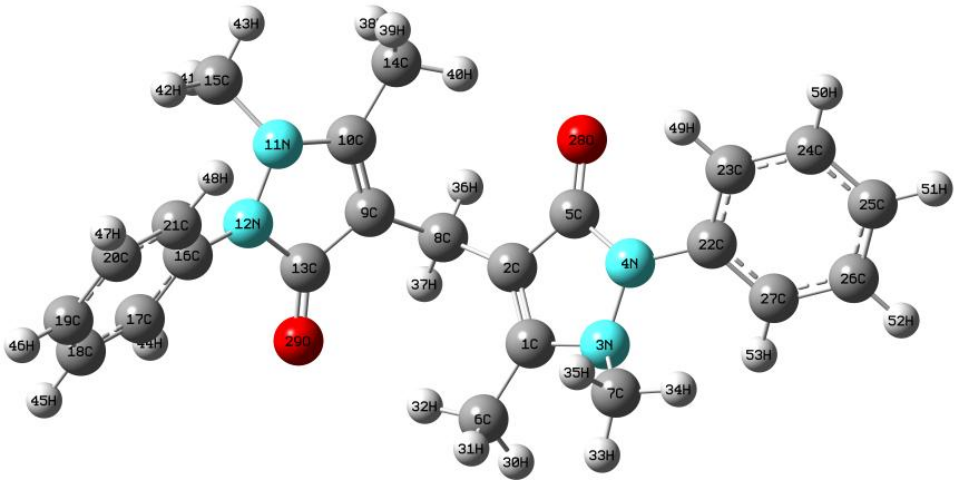

(a)

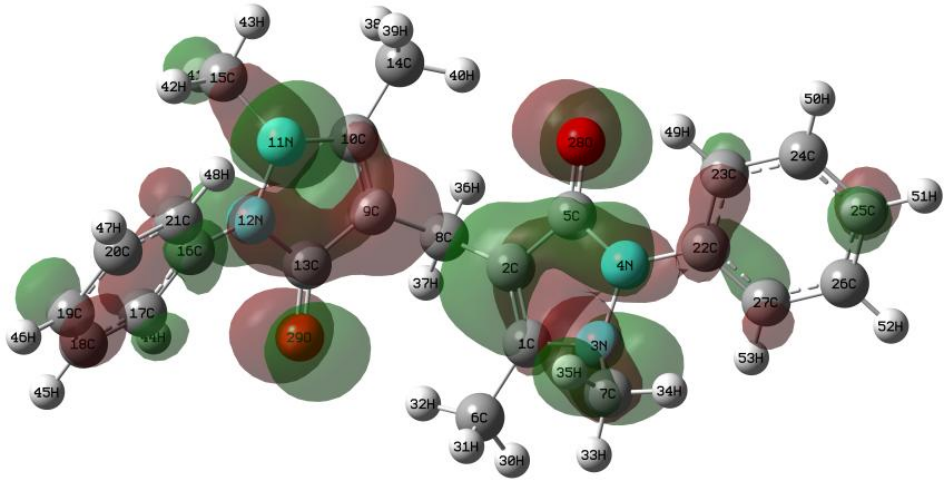

(b)

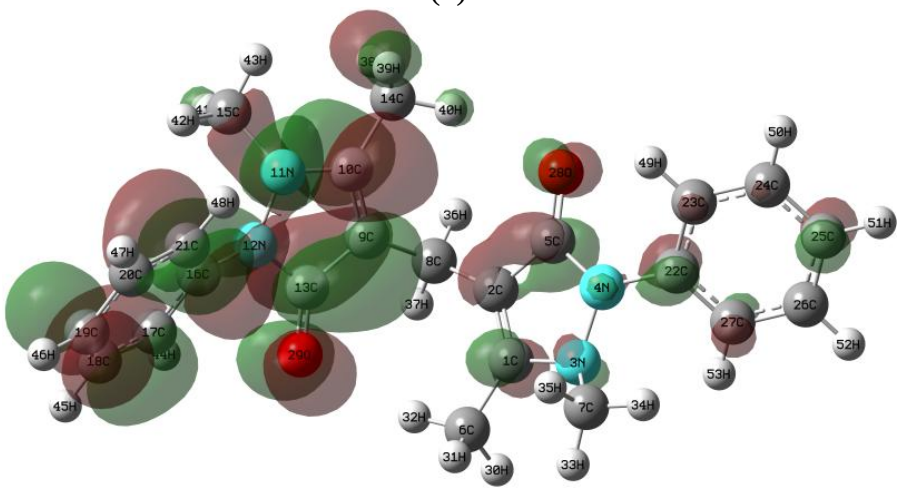

(c)

Figure 11. Optimized molecular structure (a) the distributions of HOMO (b) and the distributions of LUMO (c) of DAM with labels.

To further understand the relation between molecular structure and absorption behaviour of corrosion inhibitor, the quantum chemical calculation of was carried out. Consequently, the optimized geometric structure and the distributions of HOMO and LUMO of DAM are demonstrated in Fig. 11, moreover, the calculated Mulliken atomic charges and the calculated quantum chemical parameters containing the total energy, E_{HOMO}, E_{LUMO}, ΔE, and μ of DAM are listed in Table 5 and 6, respectively.

Table 5. Mulliken charges for representative atoms in DAM molecule

Atom	Mulliken charge	Atom	Mulliken charge	Atom	Mulliken charge	Atom	Mulliken charge
1C	0.326	9C	-0.005	17C	0.074	25C	0.017
2C	-0.003	10C	0.323	18C	-0.024	26C	-0.02
3N	-0.386	11N	-0.384	19C	0.016	27C	0.033
4N	-0.55	12N	-0.554	20C	-0.021	28O	-0.499
5C	0.5	13C	0.497	21C	0.031	29O	-0.497
6C	0.05	14C	0.045	22C	0.269		
7C	0.248	15C	0.246	23C	0.074		
8C	-0.054	16C	0.273	24C	-0.023		

Table 6. Quantum chemical parameters for DAM

E_{HOMO} (ev)	E_{LUMO} (ev)	ΔE (ev)	μ(D)	Total energy
-5.4689	-0.6177	-4.8512	2.5099	-34285.8092

It is obvious from Fig. 11 (b) and Table 5, HOMO mainly located in two pyrazolone rings containg four nitrogen atoms and two oxygen atoms with high electron densities, in this case, DAM molecule may adsorb on steel surface in acid medium by donating electrons of pyrazolone rings to the vacant d orbitals of iron [37]. In addition, contrary to the symmetric distribution of HOMO, LOMO shown in Fig. 11 (c) only focuses on one side of symmetric structure of DAM molecule, which should be explained that the asymmetric distribution of LOMO is more conducive to the formation of the optimum electron acceptor within DAM molecule[38-39].

According to the frontier molecular orbital theory, the higher value of E_{HOMO} corresponds to a good donor of the molecule, and the lower value of E_{LUMO} corresponds to a good electron acceptor of molecule, and the lower value of ΔE may represent the better stability of inhibitor molecule on the metal surface and the higher inhibition efficiency [40].

As can be seen in Table 6, the value of E_{HOMO} is high whereas the value of E_{LUMO} is low, indicating that DAM molecules can well donate electrons to the appropriate acceptor molecules on steel surface with low energy and the electron accepting ability of DAM molecule is also facile. Furthermore, the value of ΔE is not high, which implies that DAM has the good adsorption stability relating to the good inhibiting properties on mild steel surface in 0.5 M H_2SO_4 solution[40-41].

4. CONCLUSION

(1) Weight loss measurements reveal that DAM is an effective inhibitor for mild steel corrosion in 0.5 M H_2SO_4 solution, the inhibition efficiency increases with increasing DAM concentration whereas the inhibition efficiency decreases with increasing temperature.

(2) EIS measurements demonstrate that the charge transfer resistance increases and double layer capacitance declines with the increase of DAM concentration, confirming that DAM molecules can easy absorb on mild steel surface in acid medium.

(3) Polarization measurements depict that DAM is a mixed type corrosion inhibitor with more pronounced effect on anodic domain, which can simultaneously inhibit the anodic and cathodic processes of mild steel corrosion in 0.5 M H_2SO_4 solution.

(4) The adsorption of DAM on the mild steel surface in 0.5 M H_2SO_4 solution obeys the Langmuir adsorption isotherm, and the adsorption mechanism is mixed physical and chemical adsorption, and the adsorption process is an exothermic process.

(5) SEM displays a smoother surface for inhibited steel samples than uninhibited samples due to the formation of adsorption film of DAM on mild steel surface.

(6) Theoretical calculations show that DAM absorb on mild steel surface mainly by pyrazolone rings within molecular structure.

ACKNOWLEDGEMENT
This project is supported by Natural Science Foundation of China (No. 51502182), the Opening Project of Key laboratory of Material Corrosion and Protection of Sichuan Province (Nos. 2011CL13 and 2015CL04) and Scientific Research fund of Sichuan University of Science & Engineering (No. 2011KY04).

References

1. M. Finsgar, J. Jackson, *Corro. Sci*., 86 (2014) 17.
2. B.M. Mistry, S.K. Sahoo, S. Jauhari, *J. Electroanal. Chem*., 704(2013) 118.
3. H. Hamani, T. Douadi, M. Al-Noaimi, S. Issaadi, D. Daoud, S. Chafaa, *Corros. Sci*., 88(2014) 234.
4. K.G. Zhang, B. Xu, W.Z. Yang, X.S. Yin,Y. Liu, Y.Z. Chen, *Corros. Sci*., 90(2015) 284.
5. K.R. Ansari, M.A. Quraishi, A. Singh, *J. Ind. Eng. Chem*., 25(2015) 89.
6. M. Yadav, S. Kumar, R.R. Sinha,I. Bahadur, E.E. Ebenso, *J. Mol. Liq*., 211(2015) 135.
7. M. Abdallah, H.E. Meghed, M. Sobhi, *Mater. Chem. Phys*., 118 (2009) 111.
8. A.S. Fouda , G.Y. El-Ewady, S. Fathy, *Desalin. Water. Treat*., 51 (2013) 2202.
9. S.S. Abd El-Rehim, M.A.M. Ibrahim, K. F. Khaled, *J. Appl. Electrochem*., 29 (1999) 593.
10. Y. Abboud, A. Abourriche, T. Saffaj, M. Berrada, M. Charrouf, A. Bennamara, H. Hannache, *Desalination*., 237 (2009) 175.
11. K.M. Govindaraju, D. Gopi, L. Kavitha, *J. Appl. Electrochem*., 39 (2009) 2345.
12. R.M. Issa, M.K. Awad, F.M. Atlam, *Mater. Corros*., 61 (2010) 709.
13. A.U. Ezeoke, O.G. Adeyemi, O.A. Akerele, N.O. Obi-Egbedi, *Int. J. Electrochem. Sci*., 7 (2012) 534.
14. S. Sungur, *Spectrochimi. Acta. Part A*., 57(2) (2001) 349.
15. R. Caletka, V. Krivan, *Anal. Chim. Acta*., 162 (1984) 67.
16. N. O. Obi-Egbedi, I .B . Obot, *Corros. Sci*., 53 (2011) 263.
17. I.B. Obot, N.O. Obi-Egbedi, N.W. Odozi, *Corros. Sci*., 52 (2010) 923.
18. B.A. Abd-El-Naby, O. A. Abdullatef, E. Khamis, W. A. El-Mahmody, *Int. J. Electrochem. Sci*., 11 (2016) 1271.
19. P. Mourya, P. Singh, A.K. Tewar, R.B. Rastogi, M.M. Singh, *Corros. Sci*., 95 (2015) 71.
20. W. Niouri, B. Zerga, M. Sfaira1, M. Taleb, M. Ebn Touhami, B. Hammouti, M. Mcharfi1, S.S. AlDeyab, H. Benzeid, E. Essassi, *Int. J. Electrochem. Sci*., 9 (2014) 8283.
21. I. Danaee, M. Gholami, M. RashvandAvei, M.H. Maddahy, *J. Ind. Eng. Chem*., 26(2015) 81.
22. N.K. Gupta, C. Verma, M.A.Quraishi, A.K. Mukherjee, *J. Mol. Liq*., 215(2016) 47.
23. M. Yadav, S. Kumar, T. Purkait, L.O. Olasunlcanmi , I. Bahadur, E.E. Ebenso, *J. Mol. Liq*., 213(2016) 122.
24. S.A. Soliman, M.S. Metwally, S.R. Selim, M.A. Bedair, M.A. Abbas, *J. Ind. Eng. Chem*. 20 (2014) 4311.
25. M. Mobin, S. Zehra, M. Parveen, *J. Mol. Liq*., 216(2016) 598.
26. K. Ramya, K.K. Anupama, K.M.Shainy, J. Abraham, *J. Taiwan. Inst. Chem. E*., 58(2016) 517.
27. A. Doner, R. Solmaz, M. Ozcan, G. Kardas, *Corros. Sci*., 53 (2011) 2902.
28. M. Yadav，S. Kumar, T. Purlcait, L.O. Olasunkanmi, I. Bahadur,E.E. Ebenso, *J. Mol. Liq*., 213(2016) 122.
29. D. K. Yadav, B. Maiti, M. A. Quraishi, *Corros. Sci*., 52 (2010) 3586.
30. X.H. Li, X.G. Xie, *J. Taiwan. Inst. Chem. E*., 45(2014) 3033.

31. A.O. Yüce, B.D. Mert, G. Kardaş, B. Yazıcı , *Corros. Sci*. 83 (2014) 310.
32. W. H. Li, Q. H, C. L. P, B. R. H, *Electrochim. Acta*., 52 (2007) 6386.
33. D. Ozkır, K. Kayakırılmaz, E. Bayol, A.A. Gürten, F. Kandemirli, *Corro. Sci*., 56 (2012) 143.
34. R.X. Chen, L. Guo, S.Y. Xu, *Int. J. Electrochem. Sci*., 9 (2014) 6880.
35. S.M. Shaban, I. Aiad, M.M. El-Sukkary, E.A. Soliman, M.Y. El-Awady, *J. Ind. Eng. Chem*., 21 (2015) 1029.
36. A. Doner, G. Kardas, *Corro. Sci*., 53 (2011) 4223.
37. L. Li, X.H. Zhang, S.D Gong, H.X. Zhao, Y. Bai, Q.S. Li d, L. Ji., Corros. Sci. 99 (2015) 76.
38. H.J. Guadalupe, E. Garcia-Ochoa, P.J. Maldonado-Rivas, J. Cruz, T. Pandiyan., *J. Electroanal. Chem*., 655 (2011) 164.
39. H. Ju, Z.P. Kai, Y. Li, *Corros. Sci*., 50 (2008) 865.
40. G. Gece, *Corros. Sci*., 50 (2008) 2981.
41. S.A. Soliman, M.S. Metwally, S.R. Selim, M.A. Bedair, M.A. Abbas, *J. Ind. Eng. Chem*., 20 (2014) 4311.